

Region-Enhanced Feature Learning for Scene Semantic Segmentation

Xin Kang, Chaoqun Wang, Xuejin Chen

Abstract—Semantic segmentation in complex scenes not only relies on local object appearance but also on object locations and the surrounding environment. Nonetheless, it is difficult to model long-range context in the format of pairwise point correlations due to its huge computational cost for large-scale point clouds. In this paper, we propose to use regions as the intermediate representation of point clouds instead of fine-grained points or voxels to reduce the computational burden. We introduce a novel Region-Enhanced Feature Learning network (REFL-Net) that leverages region correlations to enhance the features of ambiguous points. We design a Region-based Feature Enhancement module (RFE) which consists of a Semantic-Spatial Region Extraction (SSRE) stage and a Region Dependency Modeling (RDM) stage. In the SSRE stage, we group the input points into a set of regions according to the point distances in both semantic and spatial space. In the RDM part, we explore region-wise semantic and spatial relationships via a self-attention block on region features and fuse point features with the region features to obtain more discriminative representations. Our proposed RFE module is a plug-and-play module that can be integrated with common semantic segmentation backbones. We conduct extensive experiments on ScanNetv2 and S3DIS datasets, and evaluate our RFE module with different segmentation backbones. Our REFL-Net achieves 1.8% mIoU gain on ScanNetv2 and 1.0% mIoU gain on S3DIS respectively with negligible computational cost compared to the backbone networks. Both quantitative and qualitative results show the powerful long-range context modeling ability and strong generalization ability of our REFL-Net.

Index Terms—Semantic segmentation, region extraction, region dependency modeling.

I. INTRODUCTION

Point cloud semantic segmentation plays an important role in scene understanding. This task aims to classify input points into different semantic classes. It has broad application prospects in autonomous driving, robotics, and augmented reality. During segmentation, appearances are extremely important to help identify the correct category. However, different objects may have similar local appearances, leading to confusing predictions, as shown in Figure 1 (a) and (b). This can be attributed to the fact that different furniture in indoor scenes tend to have similar components. Therefore, focusing on local features is insufficient to make robust predictions. Long-range context including location information and surrounding objects is also necessary.

Most previous methods [2]–[9] follow a down-sampling up-sampling framework to progressively aggregate multi-level

Xin Kang, Chaoqun Wang and Xuejin Chen are with the National Engineering Laboratory for Brain-inspired Intelligence Technology and Application, University of Science and Technology of China, Hefei 230026, China (e-mail: kx111@mail.ustc.edu.cn, cq14@mail.ustc.edu.cn, xjchen99@ustc.edu.cn).

Xuejin Chen is the corresponding author.

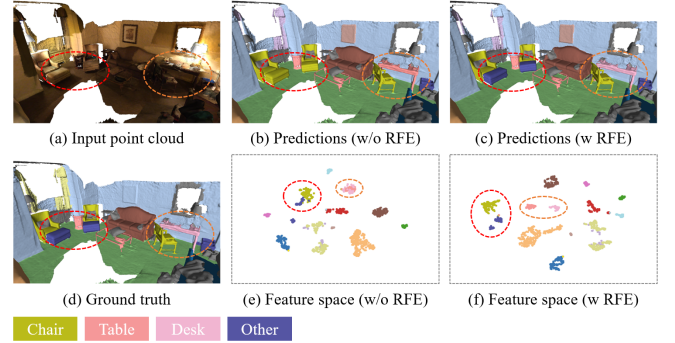


Fig. 1. Local Confusing Challenge. In (a), the footrests (red circle) belonging to ‘Other’ category have a similar texture as the ‘Chair’ and the ‘Desk’ (orange circle) has similar geometry as the ‘Table’. As shown in (b), focusing on local feature aggregation, the segmentation model can not make correct predictions. In (c), through the aim of our Region-based Feature Enhancement module, the network can well integrate long-range context, including the perception of surrounding objects and relative position in the whole scene, and make correct predictions. In (e) and (f), we visualize the feature distribution using t-SNE [1] maps. It shows that our method can learn more distinctive point features.

point features. These methods focus on how to design an effective local feature aggregation function, lacking the exploration of long-range dependencies. Along another research line, attention-based networks [10]–[12] aim to exploit long-range context in point clouds by employing self-attention on points. Since the computational cost of self-attention layers is related to the number of queries and keys, the input size and receptive field size of these methods are greatly limited. The number of input points is set to 1,024 and 2,048 separately in [10] and [11], which compromises the generalization ability to large-scale point clouds. The range of key points in Stratified Transformer [12] is limited to local regions, even with a stratified key sampling strategy. Point-level pairwise correlations in large-scale point clouds are difficult to capture under limited computational resources.

Different from previous point or voxel representations that are greatly redundant, we propose to use regions as a more compact point cloud representation, where each region stands for a group of points that are close in both semantic space and geometric space. Since the number of regions is much smaller than the number of points, we can model long-term dependencies using attention operations at a low computational cost. Much research has been done on how to partition point clouds, using uniformly divided grids [12], formulating an optimization function [13], or employing an over-segmentation network [14]. However, these methods have

some shortcomings. Grid partitioning is coarse and cannot separate points belonging to different classes. An optimizer or an over-segmentation network requires additional time to optimize or train and hurts the clustering efficiency.

In this paper, we design a plug-and-play Region-based Feature Enhancement (RFE) module that enables fast point cloud clustering and learns discriminative point features by exploring region-wise semantic and spatial relationships. Our RPE consists of two parts: the Semantic-Spatial Region Extraction (SSRE) part and Region Dependency Modeling (RDM) part. In the semantic-spatial region extraction part, we divide the input point cloud into a set of regions based on the distance between points in both semantic space and coordinate space. In detail, we first assign points into different semantic groups according to the similarity between points in the feature space. Nonetheless, semantic-level groups are too coarse to represent more detailed and complex local regions. Therefore, we further divide each semantic group into non-overlapping local regions using the k-nearest neighbors algorithm in coordinate space. By taking advantage of point features from the segmentation model, we can perform point cloud clustering faster and better without an extra over-segmentation network or optimizer. In the region dependency modeling part, we learn discriminative region features by modeling the dependencies between different regions. Firstly, we obtain region embeddings through average pooling over point features in each region. We then perform region-level self-attention, treating each region as a query, all other regions as keys and computing region association maps. Thus the effective receptive field can be enlarged to the entire scene while maintaining a low computational cost. Besides, following [12], [15], relative positional information is incorporated to enable spatial relationship capturing. Finally, we fuse point features and the corresponding region features to obtain better semantic predictions, as shown in Figure 1 (c).

As a feature augmentation tool, our Region-based Feature Enhancement module can be plugged into both point-based and voxel-based models and improve the segmentation results by capturing long-range context in large-scale point clouds. We conduct experiments on ScanNetv2 [16] and S3DIS [17] datasets, and evaluate our RFE module on multiple 3D segmentation baselines. Our REFL-Net achieves 1.8% mIoU gain on ScanNetv2 and 1.0% mIoU gain on S3DIS separately.

In summary, our contributions include the following.

- We propose the region representation to enable efficient long-range context modeling for large-scale point clouds. A region is defined as a set of points that are close in both semantic and coordinate space. Compared with points or voxels, the region representation is more compact and has fewer items, which is friendly for calculating pairwise correlations.
- We design a plug-and-play Region-based Feature Enhancement module. Our RFE module possesses powerful long-range context modeling ability by clustering points into regions and exploiting their relationships. Besides, our RFE module is plug-and-play and has a strong generalization ability to various semantic segmentation models.

- Experiments on multiple baseline models and datasets show our superiority. Our REFL-Net achieves 1.8% mIoU and 1.0% mIoU gain separately on ScanNetv2 and S3DIS datasets.

II. RELATED WORK

A. Indoor scene Semantic Segmentation

Previous semantic segmentation methods for point clouds can be mainly categorized into three categories according to the data representation: point-based methods, voxel-based methods and hybrid models. Point-based methods [2], [5], [6], [8]–[10], [12], [18]–[28] take unstructured points as input and learn multi-scale features from their color and location attributes for semantic segmentation by a down-sampling and up-sampling framework. Various feature aggregation kernels are designed for unstructured points. The key is how to assign weights to point features in the neighborhood. PointNet [18] and PointNet++ [2] use a max-pooling operation to aggregate point features hierarchically. PointCNN [5] learns a transformation matrix that weights and permutes neighboring points according to spatial distances between points. Instead of learning a permutation matrix, KPConv [19] learns correlation coefficients for different kernel points based on relative distances, and uses them to generate convolutional weights through the weighted sum. Since density inhomogeneity is common in point clouds, PointConv [6] further exploits the inverse density scale to re-weight neighboring points. Recently, similar to Vision Transformer and its wide applications in 2D images [29]–[31], several works [9], [10], [12], [32] focus on exploring feature and spatial correlations between points by applying attention operations on local neighborhood point sets. PCT [11] proposes an offset-attention module that calculates the difference between the self-attention features and the input features. Compared with original self-attention, the offset-attention can learn relative coordinate features that are invariant to rigid transformations. Besides, it formulates the optimization process as a very efficient Laplacian process. Different from PCT that performs attention on the entire point cloud, Engel et al. [10] propose to select a set of significant points for local feature learning and model relationships between local and global features through a local-global attention mechanism. Zhao et al. [9] use local self-attentions in a limited neighborhood, which requires fewer computation resources and enables the network to handle large-scale point clouds. Since local structures vary a lot and are difficult to be characterized with a single representation space, HAPGN [32] leverages a gated attention mechanism to learn different weights of neighboring points and multiple representation spaces to enhance local feature extraction. However, these attention-based models must limit the number of input points or neighborhood size due to the huge computational cost of self-attentions, which is related to the number of queries and keys. This compromises the generalization ability to large-scale point clouds. Recently, Stratified Transformer [12] introduces the Swin Architecture [33] into point cloud semantic segmentation and proposes a stratified key-sampling strategy to effectively enlarge the receptive field of attention layers

under limited computation resources. Whereas, the effective receptive field is still a local region.

Voxel-based methods [4], [7], [34], [35] take the voxelized point cloud as input. Different from the original point clouds, voxel representation greatly reduces redundant information in the same voxel grid, enabling the model to efficiently handle large-scale point clouds. To further reduce redundant computation on unoccupied voxels, sparse convolutions [7], [34] are designed for voxel feature learning. Voxel-based methods also follow a down-sampling and up-sampling framework to gradually integrate point features and lack the long-range context learning ability.

Constrained by computation resources, previous methods aggregate point or voxel features within a small local area, lacking the ability to perceive spatially distant relationships, such as the position relative to layout and surrounding objects. However, both the location information and dependencies of other objects are extremely important to learn distinctive point features. In our work, by using regions as a more compact point cloud representation, we can efficiently model long-range relationships between different regions in large-scale point clouds and enhance point features for more robust predictions.

B. Point Cloud Over-Segmentation

To reduce the redundancy of point clouds, over-segmentation task [13], [14], [36]–[38] has been investigated for many years. This task aims to generate super-points or super-voxels that provide a more compact representation for 3D points and reduce the computational cost of subsequent point cloud processing tasks. Both unsupervised and supervised models have been studied. As an unsupervised method, VCCS [13] generates super-points that conform to object boundaries by applying the local K -means clustering algorithm in a hand-crafted feature space, which consists of the spatial coordinates, colors and Fast Point Feature Histograms (FPFH) [39]. However, VCCS is not stable due to the sensitivity to initial points. To solve this problem, Lin et al. [36] formulate the over-segmentation task as a subset selection problem, which doesn't require seed points initialization. FPFH are also used as point features in [36]. Nonetheless, hand-crafted features are not representative enough to achieve good clustering results. Recently, SSP [38] proposes a supervised framework that learns point embeddings with high contrast at objects' boundaries using a novel graph-structured contrastive loss. Whereas SSP is not an end-to-end framework cause it still uses the optimization-based method in [40] to generate super-points. SPNet [14] is proposed as an end-to-end framework that learns association maps between points and super-point centers in the feature embedding space and iteratively performs clustering based on them. Compared with the optimization-based method in [40], SPNet generates super-points according to the high-dimensional feature correlations which are more robust and yield state-of-the-art results.

Different from the above methods, in this paper, we introduce a simple yet effective clustering method based on the k-nearest neighbors algorithm that generates regions by utilizing

the distances between point features and xyz coordinates. By taking advantage of point features extracted from the semantic segmentation network, we can achieve fast point cloud clustering without additional over-segmentation networks or optimization procedures.

C. Hybrid Semantic Segmentation Models

Due to the lack of fine-grained texture, geodesic information, and structural priors, point clouds are not sufficiently expressive. In order to solve this problem, recently many approaches [41]–[46] have been proposed to design hybrid models to combine additional information in multiple modalities, including images, meshes, and 3D planes. [41], [42], [44] use the projection operation to combine 2D pixel features that have more texture detail with 3D voxel features that have more geometric detail. VMNet [43] utilizes Euclidean and geodesic information in mesh representations to distinguish spatially close objects and handle irregular and complex geometries. 3D-PAM [46] is proposed to explore plane information in a scene that can both help separate touching objects close to planes and model holistic scene context between different planes. Whereas, 3D-PAM requires additional detected planes as input and lacks the context between different objects, which is also necessary to help distinguish confusing areas. In comparison, our Region-based Feature Enhancement module can model dependencies between different regions, including objects and planes, without additional geometric priors.

III. METHOD

Our REFL-Net consists of a plug-and-play module named Region-based Feature Enhancement (RFE), which can be integrated with both point- and voxel-based semantic segmentation models to explore long-range dependencies between different regions in indoor scenes. The main architecture of our REFL-Net is shown in Fig. 2. Given a point cloud as input, we first utilize a segmentation backbone that consists of an encoder to extract point features and a multi-layer perceptron (MLP) to produce the initial segmentation. Then we cluster points into a set of regions according to point semantic features and spatial coordinates in the Semantic-Spatial Region Extraction (SSRE) step. After that, we apply a self-attention block to model correlations between regions in the Region-Dependency Modeling (RDM) step. Finally, we fuse point features and corresponding region features to make per-point predictions.

A. Network Architecture

Given a point cloud $\mathcal{P} \in \mathbb{R}^{N \times 3}$ with N points associated with rgb values, the semantic segmentation task aims to predict the semantic categories of each point p_i . A base framework of semantic segmentation consists of an encoder that gradually aggregates point features, denoted as $\mathbf{F} \in \mathbb{R}^{N \times d}$, where d is the feature dimension, and applies an MLP layer over point features to get the semantic probability vector \mathbf{y}_i for point p_i .

Within the base semantic segmentation framework, the feature encoder aggregates information in a local spatial neighborhood for each point separately. Though the encoder

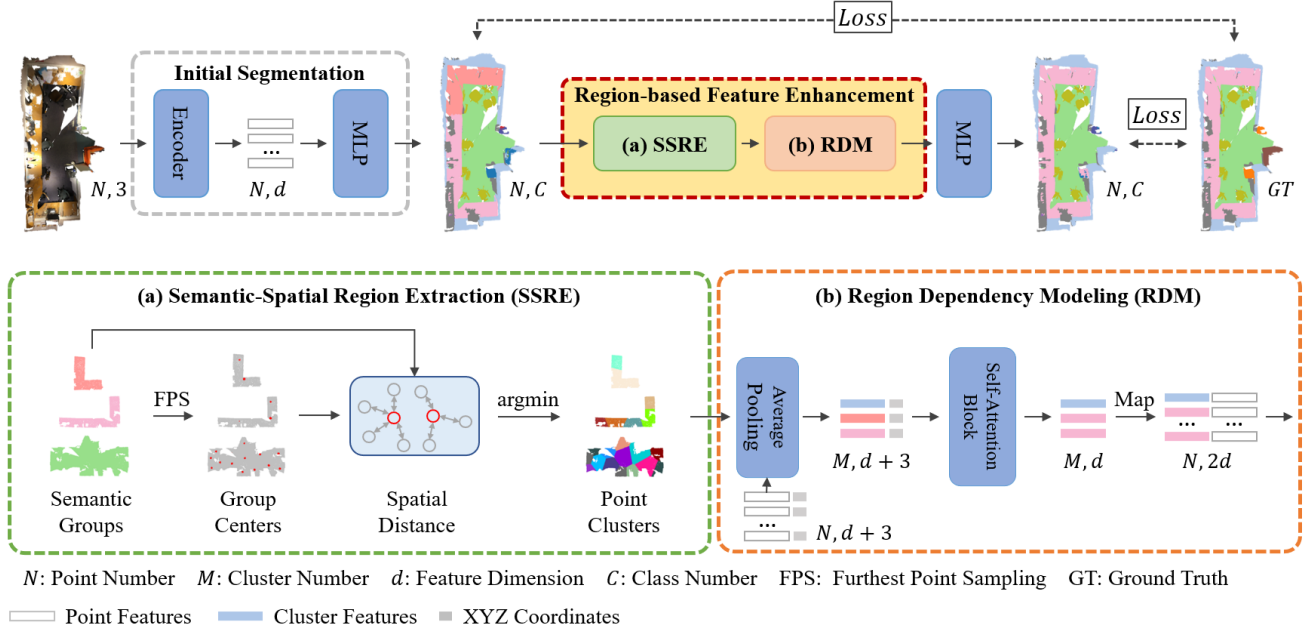


Fig. 2. Overview of our REFL-Net for point cloud semantic segmentation. With a general segmentation backbone that extracts point features and makes the initial prediction, our Region-based Feature Enhancement (RFE) module extracts region-level context to enhance the point features for better semantic segmentation. The RFE module consists of Semantic-Spatial Region Extraction (SSRE) and Region Dependency Modeling (RDM). The SSRE module takes the initial predictions as input and separates the point cloud into a set of local regions. The RDM module models the semantic and spatial correlations between regions and fuses point features and region features to make the final prediction.

can learn multi-scale features by aggregating features in local neighborhoods with increasing neighborhood size, it is non-trivial to distinguish points that have similar local geometry and appearance due to the lack of long-range context. While representing long-range dependency in the whole scene in the manner of pairwise point correlations is extremely expensive in both memory and computation, We address this confusion issue by region-based feature enhancement. Our RFE method first groups the input points into a set of regions and models the long-range dependency on the region level, which is much more efficient and robust.

Specifically, as a feature augmentation module, our RFE is appended after the semantic segmentation network, taking the predicted semantic labels \mathbf{Y} and point features \mathbf{F} as input. The output is a set of region features, noted as $\mathbf{F}_R \in \mathbb{R}^{M \times d}$. M is the number of regions. To extract regions and learn region correlations, we design a semantic-spatial region extraction (SSRE) module and a region dependency modeling (RDM) module.

B. Semantic-Spatial Region Extraction

Points in a local area usually have similar local features, which results in great redundancy and brings huge computational costs when calculating pairwise correlations. Clustering points into more compact regions can effectively reduce the number of visual items and make distant relationship modeling feasible. In this part, we over-segment the input point cloud \mathcal{P} into a set of regions $\{\mathcal{R}_1, \mathcal{R}_2, \dots, \mathcal{R}_M\}$ according to the Euclidean distance between points in both semantic and

coordinate space. By doing this, we can ensure both semantic consistency and spatial proximity in our final regions.

To achieve high-quality over-segmentation results, the final regions are required to be semantically pure [38], which means that clusters must not cross over multiple objects. In order to preserve the semantic purity, we first divide points into different semantic groups according to the semantic predictions \mathbf{Y} , containing point-wise relationships in the feature space. Specifically, we first get C semantic groups of which each group G_i contains all the points that are predicted as the i -th category. In this semantic-only grouping stage, a group might contain points that are far away in a large-scale scene. This coarse-grained grouping does not take spatial continuity into account and is too coarse to model the middle-level correlations in complex scenes. Then we further decompose each semantic group into a set of local regions considering the spatial continuity and proper region size. We adopt the furthest point sampling (FPS) [2] method in each semantic group to sample a set of points as region centers, noted as $\{\hat{\mathbf{p}}_1, \hat{\mathbf{p}}_2, \dots, \hat{\mathbf{p}}_{M_c}\}$, where M_c is the number of regions in the c -th semantic group. To ensure consistent region sizes in different scenes, we use a hyper-parameter s to control the maximum number of points in a region. Then the number of regions is determined by $M_c = \lfloor N_c/s \rfloor$, where N_c is the number of points in the c -th semantic group. Finally, we assign each point \mathbf{p}_i to the group of its nearest center $\hat{\mathbf{p}}_j$, according to the Euclidean distance in the spatial coordinate space, which is formulated as $\|\mathbf{p}_i - \hat{\mathbf{p}}_j\|_2^2$.

Through the semantic-spatial region extraction part, we can easily represent a point cloud as a set of regions, each

representing a group of points that are close in both semantic space and coordinate space. Besides, the number of regions is much less than the number of points, which enables more efficient long-range context modeling.

C. Region Dependency Modeling

After extracting a set of coarse-grained regions from the input large-scale point cloud, our region dependency modeling part explores semantic and spatial associations between different regions. Different from local feature descriptions, such global associations include the perception of both relative positions in the scene layout and surrounding co-occurring objects, which are necessary for learning discriminative point features.

To begin with, we initialize region features $F_R \in \mathbb{R}^{M \times d}$ by average pooling over the point features in each region. After that, we treat each region as a query, all other regions as keys, and compute region correlations by employing a self-attention block. It can be formulated as

$$\begin{aligned} Q &= F_R W^Q, K = F_R W^K, V = F_R W^V, \\ A &= \text{Softmax}(QK^T / \sqrt{d}), \\ \hat{F}_R &= \text{MLP}(AV), \end{aligned} \quad (1)$$

where $W^Q, W^K, W^V \in \mathbb{R}^{d \times d}$ are learnable parameters, $A \in \mathbb{R}^{M \times M}$ is the attention map, and $\hat{F}_R \in \mathbb{R}^{M \times d}$ denotes the final region features.

To take advantage of the spatial relationships, we follow [12], [15] to inject relative positional information into self-attention layers. Finally, we adopt an MLP layer to fuse point features and region features as shown in Figure 2. Through the region dependency modeling part, we can expand the effective receptive field to the entire scene, so that the final regional features can integrate relevant long-range context to help distinguish confusing regions.

Discussion on Computational Complexity. Using the regional representation, we reduce the computational complexity of the RDM part to $O(M^2)$, which is far less than the complexity $O(N \times k)$ of window attention in StratifiedFormer [12] when setting $M = \lfloor N/200 \rfloor$. N is the number of points and k denotes the window size. Besides, different from StratifiedFormer which stacks 18 window attention layers, our RDM is quite slight with only a three-layer self-attention block, which speeds up the inference process.

D. Overall Objective

To perform point cloud clustering, we first pre-train a semantic segmentation model to produce the initial predictions. Then we load the pre-trained weights and jointly train the overall model together with our Region-based Feature Enhancement module. Cross-Entropy loss is adopted as the criterion in both the pre-training and joint-training stages. Leveraging the powerful local feature extraction capability of the segmentation model and the powerful long-range dependency modeling capability of our RFE module, we achieve better segmentation performance.

IV. EXPERIMENTS

We conduct extensive experiments on different datasets to evaluate the efficiency and effectiveness of our REFL-Net by comparing a number of state-of-the-art approaches for indoor scene segmentation. Ablation studies demonstrate the long-range context modeling ability and strong generalization ability of our region-based feature enhancement module.

A. Experimental Settings

1) *Data and Metric:* We conduct experiments of point cloud segmentation on two indoor scene datasets, ScanNetv2 [16] and S3DIS [17]. The ScanNetv2 dataset contains 1,201 training scenes, 312 validation scenes, and 100 test scenes for scene semantic segmentation. There are 20 semantic categories in total. The S3DIS dataset consists of scanned point clouds of 271 rooms in six areas from three buildings. According to the general protocol [18], Area 5 is used as the test set and other areas are used as the training set, with 13 semantic categories in total. We use mean class-wise intersection over union (mIoU) as the evaluation metric for the semantic segmentation results. All experiments are performed on Tesla V100.

2) *Implementation Details:* Based on the main architecture shown in Figure 2, we have various options for the encoder, point cloud clustering module, and the region dependency modeling module. For the initial segmentation before the semantic-spatial region extraction step, we pre-train a semantic segmentation model to produce the initial predictions. Specifically, we train MinkowskiUNet34C [7] for 120k iterations by utilizing SGD optimizer with learning rate as $1e^{-1}$ and weight decay as $1e^{-4}$ respectively. The batch size is set to 10. Following StratifiedFormer [12], we use RGB values as inputs and keep the same data augmentation including random scaling, random rotation, drop color, chromatic jitter, etc. Besides, we voxelize the input point cloud with a voxel size of $0.02m$ to reduce the computational and storage burden for large-scale scenes, following previous work [7], [12].

In the region extraction step, we set the region size s to 200 points per region, leading to near 10^2 regions per scene. In the region dependency modeling module, we adopt a three-layer attention block, with the feature dimension and heads number of 128 and 8, respectively. To incorporate the spatial information of the points, we initialize three look-up tables for relative positional embedding according to Shaw et al. [15]. We set the maximum relative distance to 2m and the quantization size to 0.02m. After pre-training the initial semantic segmentation network, we jointly train the segmentation backbone and the region dependency modeling module. We use the SGD optimizer with learning rate as $5e^{-3}$ and $5e^{-4}$ for the segmentation model and region dependency modeling module respectively. We use a batch size of 4. We also implement a learning rate warm-up process with 3,000 iterations to keep the training process more stable.

B. Comparison with State-of-the-art Methods

We compare our method with previous works [2], [6], [8], [19], [34] and state-of-the-art methods Mix3D [47], StratifiedFormer [12], PointTransformer [11], and MinkowskiNet [7]

TABLE I
SEMANTIC SEGMENTATION mIoU(%) ON THE SCANNetV2 VALIDATION
SET AND S3DIS AREA 5.

Methods	ScanNetv2	S3DIS	Time (s)
PointNet++ [2]	53.5	-	-
PointConv [6]	61.0	-	-
PointASNL [8]	63.5	-	-
KPConv [19]	69.2	67.3	118
SparseConvNet [4]	69.3	-	-
Mix3D [47]	73.6	65.4	-
StratifiedFormer [12]	74.3	72.0	1,821
PointTransformer [9]	70.6	70.4	784
REFL-Net-PT	-	<u>71.4</u>	1,055
MinkowskiNet [7]	72.2	65.8	82
REFL-Net-Mink	<u>74.0</u>	66.9	217

and report the segmentation results in Table I. Besides mIoUs, we also report the average inference time on a Tesla V100 for each scene that contains approximately 100k points for efficiency evaluation.

We implement two variants, REFL-Net-Mink and REFL-Net-PT, of our REFL-Net using two segmentation backbones (MinkowskiNet [7] and PointTransformer [9]). On the ScanNetv2 validation set, our REFL-Net-Mink obtains comparable mIoU (74.0%) with the state-of-the-art result (74.3%) of StratifiedFormer [12], with 9× speedup. Compared with StratifiedFormer which directly uses window-based attention on points, our REFL-Net performs self-attention on regions, which is much more efficient but may neglect some details and result in a slight performance gap. Our REFL-Net-PT, which integrates the proposed RFE module with PointTransformer, obtains 1.0% mIoU gain on the S3DIS Area 5. We do not test REFL-Net-PT on ScanNetv2 since the training codes for PointTransformer are not available. The performance gains of the two REFL-Net variants compared with the backbone segmentation networks are benefited from the proposed region-based feature enhancement module, which can capture the long-range dependencies in a scene and learn more distinctive point features. We further visualize the semantic segmentation error maps in Fig. 3. As shown in Fig. 3 (b), the refrigerators in the first two scenes and the bookshelf in the third scene are classified by mistake using MinkowskiNet only due to their indistinguishable local appearances. Utilizing our RFE module, our REFL-Net significantly reduces the prediction errors by sensing more surrounding environments, as shown in Fig. 3 (c).

C. Generalization Ability of RFE Module

Our Region-based Feature Enhancement module can be plugged into most semantic segmentation models. To demonstrate its generalizability, we conduct experiments by appending RFE module after different semantic segmentation backbones and show the results in Table II.

Typically, point-based methods [9], [19] work better than voxel-based methods [7]. For point-based methods, we select KPConv [19] and Point Transformer [9] as backbone models and conduct semantic segmentation on S3DIS dataset. For a fair comparison, we adopt the same data augmentation ways as the corresponding backbone models. As shown in the last two

TABLE II
PERFORMANCE IMPROVEMENTS BY COMBINING OUR REGION-BASED
FEATURE ENHANCEMENT WITH DIFFERENT BACKBONE MODELS.

Methods	Dataset	mIoU(%)
MinkowskiUNet34C [7]	ScanNetv2	72.2
+ Our RFE	ScanNetv2	73.4
MinkowskiUNet18 [7]	S3DIS	65.8
+ Our RFE	S3DIS	66.5
KPConv(deform) [19]	S3DIS	67.3
+ Our RFE	S3DIS	67.7
PointTransformer [9]	S3DIS	70.4
+ Our RFE	S3DIS	71.4

TABLE III
EFFECT OF DIFFERENT COMPONENTS IN RFE MODULE. SeRE AND SpRE
DENOTE SEMANTIC REGION EXTRACTION AND SPATIAL REGION
EXTRACTION RESPECTIVELY. RDM IS THE REGION DEPENDENCY
MODELING PART AND RPE DENOTES THE RELATIVE POSITIONAL
ENCODING.

EXP	SeRE	SpRE	RDM w/o RPE	RDM w RPE	mIoU (%)
I					72.22
II	✓				72.37
III		✓			72.37
IV	✓	✓			72.80
V	✓	✓	✓		73.07
VI	✓	✓		✓	73.41

rows of Table II, our RFE module brings 0.4% and 1.0% mIoU gains for KPConv [19] and Point Transformer [9] respectively. Although KPConv and PointTransformer consider point-wise correlations through deformable convolutions or self-attention, they work in local neighborhoods, making it hard to effectively learn long-range context. In comparison, our region-based representation and dependency modeling method bring the benefit of perceiving location and surrounding environment information and learning more distinctive features. For voxel-based methods, we choose MinkowskiNet [7] as the backbone for its high performance and efficiency. We conduct semantic segmentation on both ScanNetv2 and S3DIS datasets and results are shown in the first two rows of Table II. 1.2% and 0.7% mIoU gains are achieved for the two datasets respectively, showing the effectiveness of our REF module in capturing long-range context in complex scenes.

D. Ablation Study

1) *Analysis of Different Components in RFE Module:* To demonstrate the importance of the semantic-spatial region extraction part and region dependency modeling part in our RFE module, we conduct a set of experiments on ScanNetv2 dataset and results are shown in Table III.

To analyze the effects of different components of the SSRE part, we adopt different clustering strategies after the semantic segmentation model in EXP II, III and IV. EXP I serves as the baseline experiment which adopts the MinkowskiNet for semantic segmentation. EXP II uses semantic region extraction and gets 0.15% mIoU gain. This is because the final region features represent the semantic centers of different categories, which keep the point features away from the classification plane, making them easier to classify. EXP III adopts spatial region extraction and gets 0.15% mIoU gain. This improvement can be attributed to the local consistency constraint,

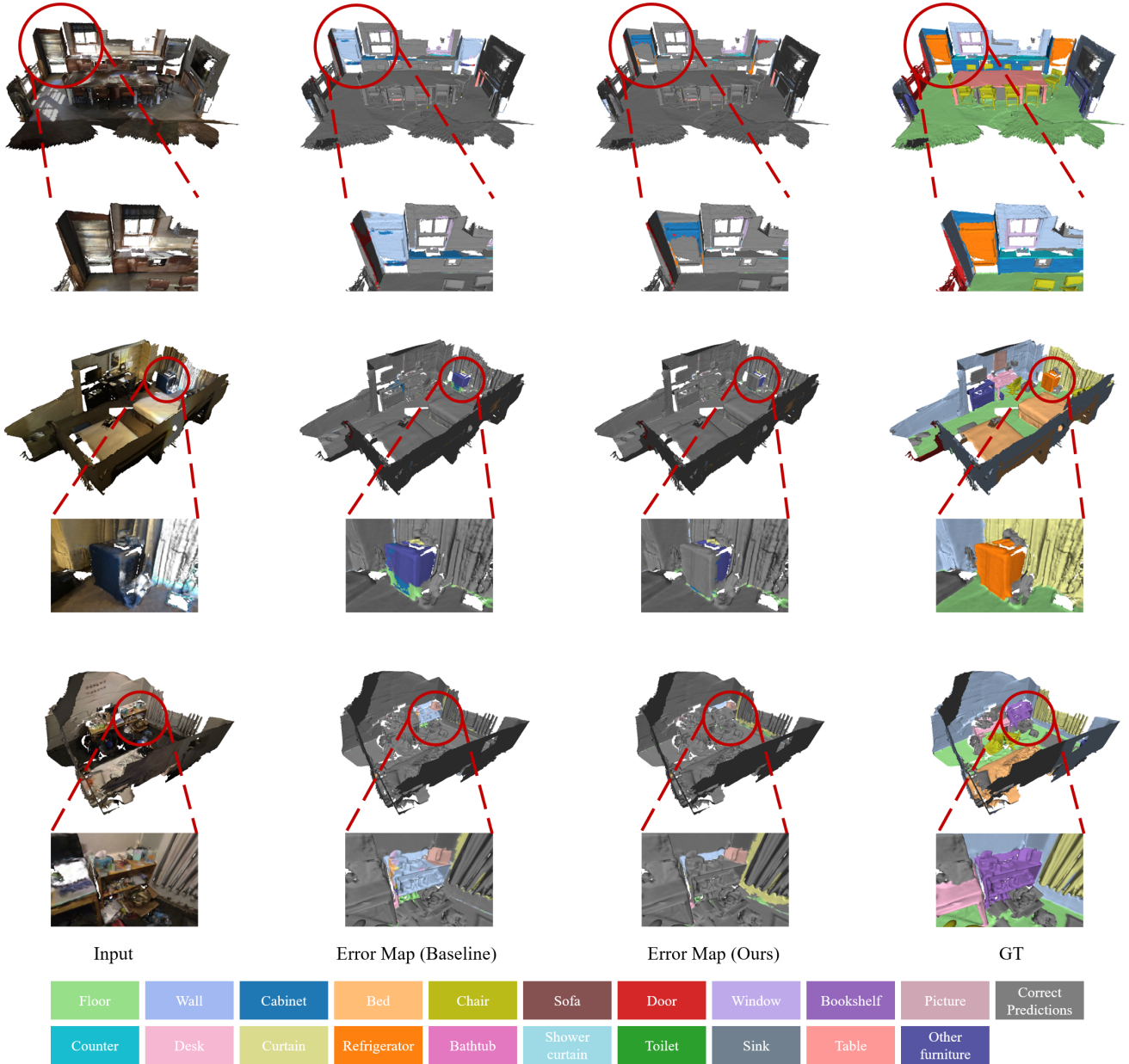


Fig. 3. Semantic segmentation errors on three indoor scenes in ScanNetv2. (a) The input point clouds. We visualize the semantic segmentation errors (colored points) of MinkowskiNet [7] and our REFL-Net in (b) and (c) respectively. Grey points in (b)(c) have correct predictions compared with the Ground-Truth (d).

which forces points in the same local region to have similar features and makes predictions smoother. In EXP IV, we use semantic and spatial region extraction sequentially and achieve 0.58% mIoU gain. The improvement by semantic region extraction or spatial region extraction alone is limited. This is because the semantic subdivision is too coarse and may assign points to the wrong class. And spatial region extraction cannot separate adjacent points belonging to different categories without semantic information. By combining both of them, we can generate better clusters, each containing a set of points that are close in both feature space and coordinate space.

To analyze the effect of region dependency modeling, we employ the RDM part after region extraction and results are shown in EXP V and VI. Compare with EXP IV that directly fuse cluster features with point features after point cloud clustering, EXP VI further appends the RDM part after the point cloud clustering part to explore correlations between clusters. By fusing point features with cluster features containing long-range context, it achieves 0.61% mIoU gain compared with EXP IV. In addition, in EXP V, we evaluate the effect of relative positional encoding which can help learn spatially correlations. It still gains 0.27% mIoU compared with EXP IV and demonstrates the importance of long-range

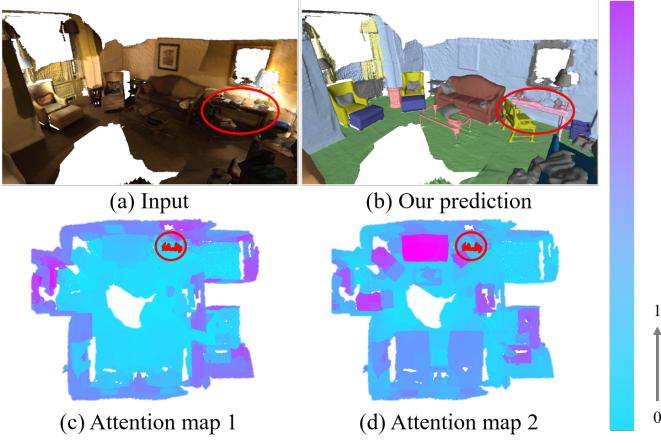


Fig. 4. Attention map visualization. The query region is indicated in red circle. (c) shows the attention map of the scene layout. (d) shows the attention map of surrounding objects.

context modeling.

2) *Attention Map Visualization*: To verify the long-range context modeling ability of the RDM part, we visualize the attention maps of the self-attention layers, which represent correlations between different regions. Given the query region noted by a red circle, we select two representative attention maps to show the perception of scene layout and surrounding objects in Figure 4 (c) and (d) respectively. Purple indicates higher attention weights, and blue indicates lower attention weights. In Figure 4 (c), the ‘desk’ region has higher attention weights to ‘wall’ representing the horizontal layout, which helps to perceive its position in the scene. Relative positions of the same object in different indoor scenes usually have similarities and can help distinguish. In Figure 4 (d), the ‘desk’ region has higher attention weights to other objects including ‘sofa’ and ‘chair’, revealing co-occurring dependencies between different furniture in indoor scenes. This dependency can provide more accurate information about objects. Attention maps in Figure 4 show that our RDM can effectively model long-range context in indoor scenes and learn more discriminative region features.

3) *Point cloud Over-Segmentation*: We also compare different point cloud over-segmentation methods in Table IV, including our SSRE and the state-of-the-art SPNet [14]. Since the number of generated clusters can be deterministically specified for either of the two clustering methods, we set the super-point ratio to 0.002 for SPNet and the region size to 200 for SSRE to ensure a comparable number of clusters. To measure the clustering performance, we calculate the average cluster entropy and boundary recall [14] on ScanNetv2 validation set. The cluster entropy reflects the semantic purity for each cluster and is formulated as,

$$E(c_j) = - \sum_{i=1}^C p_i \log(p_i), \quad (2)$$

where p_i denotes the ratio of points belonging to the i -th class in each cluster c_j and C is the total number of semantic classes. To measure the semantic purity of clustering results

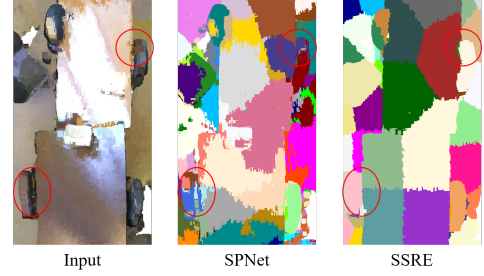


Fig. 5. Point cloud clustering. Given an input point cloud, we visualize the clustering results using SPNet [14] and our Semantic-Spatial Region Extraction (SSRE).

TABLE IV
COMPARISON OF DIFFERENT POINT CLOUD CLUSTERING METHODS ON THE VALIDATION SET OF SCANNETV2. SSRE DENOTES THE SEMANTIC-SPATIAL REGION EXTRACTION. BR DENOTES BOUNDARY RECALL.

Method	# Cluster	Entropy	BR (%)	mIoU (%)
SPNet [14]	318	0.185	67.78	73.10
SSRE	278	0.112	68.80	73.41

on the entire validation set, we compute the average cluster entropy across different scenes and clusters following

$$E_{val} = \frac{1}{N_S} \sum_{i=1}^{N_S} \left(\frac{1}{M_i} \sum_{j=1}^{M_i} E(c_{ij}) \right), \quad (3)$$

where N_S denotes the number of scenes in the validation set and M_i is the number of clusters in the i -th scene. Boundary recall is computed in each scene and averaged over the validation set. In comparison with SPNet, our SSRE is easy to transfer to various segmentation models and requires no additional training on over-segmentation tasks. So that we can benefit from a powerful feature extractor and obtain better clustering results, which are visualized in Figure 5. As Table IV shows, we achieve 0.88% and 1.19% mIoU gains by using our RFE module with SPNet and SSRE, respectively, compared with the 72.22% mIoU of MinkowskiNet. This shows the generalization ability of our region-based feature enhancement framework to different clustering methods.

4) *Analysis of Region Size*: In the semantic-spatial region extraction part, the region size s serves as a hyper-parameter and controls the maximum number of points in final clusters. We analyze the influence of different values of region size and the results on ScanNetv2 validation set are shown in Table V. With region size set to 100 and 200, we get 0.56% and 1.19% mIoU gain respectively, compared with the baseline model. Because a smaller region size results in more regions and correspondingly more complex, harder-to-capture correlations, the former improvement is less than the latter. As the region size increases to 300 and 400, improvements become smaller (0.67% and 0.60%), as larger regions sacrifice more detail and limit segmentation performance. In our final model, we set each region to contain up to 200 points for the best result.

5) *Analyze the Number of Attention Layers*: In the region dependency modeling part, we utilize self-attention layers to explore correlations between regions. In order to determine

TABLE V
ANALYSIS OF REGION SIZE ON SCANNETV2 VALIDATION SET.

Region size	-	100	200	300	400
mIoU (%)	72.22	72.78	73.41	72.89	72.82

TABLE VI
ANALYZE THE NUMBER OF ATTENTION LAYERS.

# Attention Layer	1	2	3	4	5
# Layer Param. (M)	0.6	1.2	1.8	2.4	3.0
Time (s)	1.7	3.7	5.0	6.7	8.5
mIoU (%)	72.95	73.28	73.41	73.07	73.00

a proper number of self-attention layers, we conduct several experiments on ScanNetv2 validation set and the results are shown in Table VI. As the number of self-attention layers increases from 1 to 3, the mIoU gets higher from 72.95% to 73.41% due to the stronger modeling ability. However, when there are too many self-attention layers, the self-attention block becomes over-fitting and the modeling ability is limited, resulting in mIoUs of 73.07% and 73.00% respectively. We also measure the model size and the average inference time for each scene that contains approximately 100k points. The results in the second row of Table VI show that the attention block is lightweight and fast. In our final model, we choose to use a three-layer attention block to get the best result.

V. CONCLUSION

In this paper, we introduce a feature enhancement framework with coarse-grained regions to enhance point features, especially for indistinguishable points in complex scenes. As a key component of our REFL-Net, the proposed region-based feature enhancement module extracts local regions as the intermediate representation and models long-range region dependencies to augment point features. With the proposed region representation, our REF module effectively models long-range context in large-scale indoor scenes and achieves significant improvements with much less memory and computation cost than point-wise correlations. As a plug-and-play module, our RFE can be flexibly integrated with various semantic segmentation backbones, including both point-based and voxel-based networks. A future direction is to extend our region-based feature enhancement framework to semantic segmentation of high-resolution images or high-volume videos to capture object correlations in a more efficient manner.

REFERENCES

- [1] L. Van der Maaten and G. Hinton, "Visualizing data using t-sne." *Journal of machine learning research*, vol. 9, no. 11, 2008.
- [2] C. R. Qi, L. Yi, H. Su, and L. J. Guibas, "Pointnet++: Deep hierarchical feature learning on point sets in a metric space," *Advances in neural information processing systems*, vol. 30, 2017.
- [3] P.-S. Wang, Y. Liu, Y.-X. Guo, C.-Y. Sun, and X. Tong, "O-cnn: Octree-based convolutional neural networks for 3d shape analysis," *ACM Transactions On Graphics (TOG)*, vol. 36, no. 4, pp. 1–11, 2017.
- [4] B. Graham, M. Engelcke, and L. Van Der Maaten, "3d semantic segmentation with submanifold sparse convolutional networks," in *Proceedings of the IEEE conference on computer vision and pattern recognition*, 2018, pp. 9224–9232.
- [5] Y. Li, R. Bu, M. Sun, W. Wu, X. Di, and B. Chen, "Pointcnn: Convolution on x-transformed points," *Advances in neural information processing systems*, vol. 31, 2018.

- [6] W. Wu, Z. Qi, and L. Fuxin, "Pointconv: Deep convolutional networks on 3d point clouds," in *Proceedings of the IEEE/CVF Conference on Computer Vision and Pattern Recognition*, 2019, pp. 9621–9630.
- [7] C. Choy, J. Gwak, and S. Savarese, "4d spatio-temporal convnets: Minkowski convolutional neural networks," in *Proceedings of the IEEE/CVF Conference on Computer Vision and Pattern Recognition*, 2019, pp. 3075–3084.
- [8] X. Yan, C. Zheng, Z. Li, S. Wang, and S. Cui, "Pointasnl: Robust point clouds processing using nonlocal neural networks with adaptive sampling," in *Proceedings of the IEEE/CVF Conference on Computer Vision and Pattern Recognition*, 2020, pp. 5589–5598.
- [9] H. Zhao, L. Jiang, J. Jia, P. H. Torr, and V. Koltun, "Point transformer," in *Proceedings of the IEEE/CVF International Conference on Computer Vision*, 2021, pp. 16259–16268.
- [10] N. Engel, V. Belagiannis, and K. Dietmayer, "Point transformer," *IEEE Access*, vol. 9, pp. 134 826–134 840, 2021.
- [11] M.-H. Guo, J.-X. Cai, Z.-N. Liu, T.-J. Mu, R. R. Martin, and S.-M. Hu, "Pct: Point cloud transformer," *Computational Visual Media*, vol. 7, no. 2, pp. 187–199, 2021.
- [12] X. Lai, J. Liu, L. Jiang, L. Wang, H. Zhao, S. Liu, X. Qi, and J. Jia, "Stratified transformer for 3d point cloud segmentation," in *Proceedings of the IEEE/CVF Conference on Computer Vision and Pattern Recognition*, 2022, pp. 8500–8509.
- [13] J. Papon, A. Abramov, M. Schoeler, and F. Worgotter, "Voxel cloud connectivity segmentation-supervoxels for point clouds," in *Proceedings of the IEEE conference on computer vision and pattern recognition*, 2013, pp. 2027–2034.
- [14] L. Hui, J. Yuan, M. Cheng, J. Xie, X. Zhang, and J. Yang, "Superpoint network for point cloud oversegmentation," in *Proceedings of the IEEE/CVF International Conference on Computer Vision*, 2021, pp. 5510–5519.
- [15] P. Shaw, J. Uszkoreit, and A. Vaswani, "Self-attention with relative position representations," *arXiv preprint arXiv:1803.02155*, 2018.
- [16] A. Dai, A. X. Chang, M. Savva, M. Halber, T. Funkhouser, and M. Nießner, "ScanNet: Richly-annotated 3d reconstructions of indoor scenes," in *Proceedings of the IEEE conference on computer vision and pattern recognition*, 2017, pp. 5828–5839.
- [17] I. Armeni, O. Sener, A. R. Zamir, H. Jiang, I. Brilakis, M. Fischer, and S. Savarese, "3d semantic parsing of large-scale indoor spaces," in *Proceedings of the IEEE conference on computer vision and pattern recognition*, 2016, pp. 1534–1543.
- [18] C. R. Qi, H. Su, K. Mo, and L. J. Guibas, "Pointnet: Deep learning on point sets for 3d classification and segmentation," in *Proceedings of the IEEE conference on computer vision and pattern recognition*, 2017, pp. 652–660.
- [19] H. Thomas, C. R. Qi, J.-E. Deschaud, B. Marcotegui, F. Goulette, and L. J. Guibas, "Kpconv: Flexible and deformable convolution for point clouds," in *Proceedings of the IEEE/CVF international conference on computer vision*, 2019, pp. 6411–6420.
- [20] Y. Wang, Y. Sun, Z. Liu, S. E. Sarma, M. M. Bronstein, and J. M. Solomon, "Dynamic graph cnn for learning on point clouds," *ACM Transactions On Graphics (tog)*, vol. 38, no. 5, pp. 1–12, 2019.
- [21] Q. Hu, B. Yang, L. Xie, S. Rosa, Y. Guo, Z. Wang, N. Trigoni, and A. Markham, "Randla-net: Efficient semantic segmentation of large-scale point clouds," in *Proceedings of the IEEE/CVF Conference on Computer Vision and Pattern Recognition*, 2020, pp. 11 108–11 117.
- [22] F. Engelmann, T. Kontogianni, and B. Leibe, "Dilated point convolutions: On the receptive field size of point convolutions on 3d point clouds," in *2020 IEEE International Conference on Robotics and Automation (ICRA)*. IEEE, 2020, pp. 9463–9469.
- [23] Z. Hu, M. Zhen, X. Bai, H. Fu, and C.-I. Tai, "Jsenet: Joint semantic segmentation and edge detection network for 3d point clouds," in *European Conference on Computer Vision*. Springer, 2020, pp. 222–239.
- [24] H. Lei, N. Akhtar, and A. Mian, "Seggcn: Efficient 3d point cloud segmentation with fuzzy spherical kernel," in *Proceedings of the IEEE/CVF Conference on Computer Vision and Pattern Recognition*, 2020, pp. 11 611–11 620.
- [25] S. Fan, Q. Dong, F. Zhu, Y. Lv, P. Ye, and F.-Y. Wang, "Scf-net: Learning spatial contextual features for large-scale point cloud segmentation," in *Proceedings of the IEEE/CVF Conference on Computer Vision and Pattern Recognition*, 2021, pp. 14 504–14 513.
- [26] M. Xu, R. Ding, H. Zhao, and X. Qi, "Paconv: Position adaptive convolution with dynamic kernel assembling on point clouds," in *Proceedings of the IEEE/CVF Conference on Computer Vision and Pattern Recognition*, 2021, pp. 3173–3182.

- [27] L. Tang, Y. Zhan, Z. Chen, B. Yu, and D. Tao, "Contrastive boundary learning for point cloud segmentation," in *Proceedings of the IEEE/CVF Conference on Computer Vision and Pattern Recognition*, 2022, pp. 8489–8499.
- [28] H. Ran, J. Liu, and C. Wang, "Surface representation for point clouds," in *Proceedings of the IEEE/CVF Conference on Computer Vision and Pattern Recognition*, 2022, pp. 18 942–18 952.
- [29] A. Dosovitskiy, L. Beyer, A. Kolesnikov, D. Weissenborn, X. Zhai, T. Unterthiner, M. Dehghani, M. Minderer, G. Heigold, S. Gelly *et al.*, "An image is worth 16x16 words: Transformers for image recognition at scale," *arXiv preprint arXiv:2010.11929*, 2020.
- [30] X. Yue, S. Sun, Z. Kuang, M. Wei, P. H. Torr, W. Zhang, and D. Lin, "Vision transformer with progressive sampling," in *Proceedings of the IEEE/CVF International Conference on Computer Vision*, 2021, pp. 387–396.
- [31] W. Wang, E. Xie, X. Li, D.-P. Fan, K. Song, D. Liang, T. Lu, P. Luo, and L. Shao, "Pyramid vision transformer: A versatile backbone for dense prediction without convolutions," in *Proceedings of the IEEE/CVF International Conference on Computer Vision*, 2021, pp. 568–578.
- [32] C. Chen, S. Qian, Q. Fang, and C. Xu, "Hapgn: Hierarchical attentive pooling graph network for point cloud segmentation," *IEEE Transactions on Multimedia*, vol. 23, pp. 2335–2346, 2021.
- [33] Z. Liu, Y. Lin, Y. Cao, H. Hu, Y. Wei, Z. Zhang, S. Lin, and B. Guo, "Swin transformer: Hierarchical vision transformer using shifted windows," in *Proceedings of the IEEE/CVF International Conference on Computer Vision*, 2021, pp. 10 012–10 022.
- [34] B. Graham, "Sparse 3d convolutional neural networks," *arXiv preprint arXiv:1505.02890*, 2015.
- [35] B. Graham and L. van der Maaten, "Submanifold sparse convolutional networks," *arXiv preprint arXiv:1706.01307*, 2017.
- [36] Y. Lin, C. Wang, D. Zhai, W. Li, and J. Li, "Toward better boundary preserved supervoxel segmentation for 3d point clouds," *ISPRS journal of photogrammetry and remote sensing*, vol. 143, pp. 39–47, 2018.
- [37] L. Landrieu and M. Simonovsky, "Large-scale point cloud semantic segmentation with superpoint graphs," in *Proceedings of the IEEE conference on computer vision and pattern recognition*, 2018, pp. 4558–4567.
- [38] L. Landrieu and M. Boussaha, "Point cloud oversegmentation with graph-structured deep metric learning," in *Proceedings of the IEEE/CVF Conference on Computer Vision and Pattern Recognition*, 2019, pp. 7440–7449.
- [39] R. B. Rusu, N. Blodow, and M. Beetz, "Fast point feature histograms (fpfh) for 3d registration," in *2009 IEEE international conference on robotics and automation*. IEEE, 2009, pp. 3212–3217.
- [40] S. Guinard and L. Landrieu, "Weakly supervised segmentation-aided classification of urban scenes from 3d lidar point clouds," in *ISPRS Workshop 2017*, 2017.
- [41] A. Dai and M. Nießner, "3dmv: Joint 3d-multi-view prediction for 3d semantic scene segmentation," in *Proceedings of the European Conference on Computer Vision (ECCV)*, 2018, pp. 452–468.
- [42] W. Hu, H. Zhao, L. Jiang, J. Jia, and T.-T. Wong, "Bidirectional projection network for cross dimension scene understanding," in *Proceedings of the IEEE/CVF Conference on Computer Vision and Pattern Recognition*, 2021, pp. 14 373–14 382.
- [43] Z. Hu, X. Bai, J. Shang, R. Zhang, J. Dong, X. Wang, G. Sun, H. Fu, and C.-L. Tai, "Vmnet: Voxel-mesh network for geodesic-aware 3d semantic segmentation," in *Proceedings of the IEEE/CVF International Conference on Computer Vision*, 2021, pp. 15 488–15 498.
- [44] Z. Wang, Y. Rao, X. Yu, J. Zhou, and J. Lu, "Semaffinet: Semantic-affine transformation for point cloud segmentation," in *Proceedings of the IEEE/CVF Conference on Computer Vision and Pattern Recognition*, 2022, pp. 11 819–11 829.
- [45] D. Robert, B. Vallet, and L. Landrieu, "Learning multi-view aggregation in the wild for large-scale 3d semantic segmentation," in *Proceedings of the IEEE/CVF Conference on Computer Vision and Pattern Recognition*, 2022, pp. 5575–5584.
- [46] T. Weng, J. Xiao, F. Yan, and H. Jiang, "Context-aware 3d point cloud semantic segmentation with plane guidance," *IEEE Transactions on Multimedia*, pp. 1–12, 2022.
- [47] A. Nekrasov, J. Schult, O. Litany, B. Leibe, and F. Engelmann, "Mix3d: Out-of-context data augmentation for 3d scenes," in *2021 International Conference on 3D Vision (3DV)*. IEEE, 2021, pp. 116–125.